

On load dependence of detachment rate of kinesin motor

Xiao-Xuan Shi(史晓璇), Yao Wang(王瑶), Yu-Ru Liu(刘玉如), and Ping Xie(谢平)

Citation: Chin. Phys. B, 2025, 34 (**1**): 018702. DOI: 10.1088/1674-1056/ad8ec7

What follows is a list of articles you may be interested in

Origin of tradeoff between movement velocity and attachment duration of kinesin motor on a microtubule

Yuying Liu(刘玉颖) and Zhiqiang Zhang(张志强)
Chin. Phys. B, 2024, 33 (**2**): 028708. DOI: 10.1088/1674-1056/ad1177

Kinesin-microtubule interaction reveals the mechanism of kinesin-1 for discriminating the binding site on microtubule

Yi-Zhao Geng(耿轶钊), Li-Ai Lu(鲁丽爱), Ning Jia(贾宁), Bing-Bing Zhang(张冰冰), and Qing Ji(纪青)
Chin. Phys. B, 2023, 32 (**10**): 108701. DOI: 10.1088/1674-1056/acdfc1

Investigation of the structural and dynamic basis of kinesin dissociation from microtubule by atomistic molecular dynamics simulations

Jian-Gang Wang(王建港), Xiao-Xuan Shi(史晓璇), Yu-Ru Liu(刘玉如), Peng-Ye Wang(王鹏业),Hong Chen(陈洪), and Ping Xie(谢平)
Chin. Phys. B, 2022, 31 (**5**): 058702. DOI: 10.1088/1674-1056/ac598b

Protection-against-water-attack determined difference between strengths of backbone hydrogen bonds in kinesin's neck zipper region

Jing-Yu Qin(覃静宇), Yi-Zhao Geng(耿轶钊), Gang Lü(吕刚), Qing Ji(纪青), Hai-Ping Fang(方海平)
Chin. Phys. B, 2018, 27 (**2**): 028704. DOI: 10.1088/1674-1056/27/2/028704

Initial conformation of kinesin’s neck linker

Geng Yi-Zhao (耿轶钊), Ji Qing (纪青), Liu Shu-Xia (刘书霞), Yan Shi-Wei (晏世伟)
Chin. Phys. B, 2014, 23 (**10**): 108701. DOI: 10.1088/1674-1056/23/10/108701

On load dependence of detachment rate of kinesin motor

Xiao-Xuan Shi(史晓璇)[1], Yao Wang(王瑶)[2], Yu-Ru Liu(刘玉如)[2], and Ping Xie(谢平)[2,†]

[1] *School of Pharmaceutical Engineering, Chongqing Chemical Industry Vocational College, Chongqing* 401220, *China*
[2] *Laboratory of Soft Matter Physics, Institute of Physics, Chinese Academy of Sciences, Beijing* 100190, *China*

(Received 13 September 2024; revised manuscript received 12 October 2024; accepted manuscript online 5 November 2024)

Kinesin is an archetypal microtubule-based molecular motor that can generate force to transport cargo in cells. The load dependence of the detachment rate is an important factor of the kinesin motor, the determination of which is critically related to the chemomechanical coupling mechanism of the motor. Here, we use three models for the load dependence of the detachment rate of the kinesin motor to study theoretically and numerically the maximal force generated and microtubule-attachment duration of the motor. By comparing the theoretical and numerical results with the available experimental data, we show that only one model can explain well the available experimental data, indicating that only this model can be applicable to the kinesin motor.

Keywords: kinesin, detachment rate, generated force, chemomechanical coupling mechanism, optical trapping

PACS: 87.10.Tf, 87.15.A–, 87.15.hg

DOI: 10.1088/1674-1056/ad8ec7 **CSTR:** 32038.14.CPB.ad8ec7

1. Introduction

Kinesin-1 is a well-studied ATPase-driven molecular motor that can step on microtubule (MT) toward the plus end (forward direction) for a long distance (defined as the run length) until it detaches from MT.[1–7] The velocity, run length, detachment rate, etc., are important quantities to characterize its dynamics.[8–12] To determine these quantities and the force dependences of these quantities, the single molecule optical trapping method was usually employed, where a large-sized bead is attached to the stalk of the motor.[13–22] In the optical trapping experiment, either a movable trap ensuring a 'constant' load on the moving motor or a fixed trap was used.[13–31]

The available optical trapping data for Drosophila kinesin showed that its velocity decreases with the increase in the magnitude of the backward load, while the variation of the forward load has no effect on its velocity.[21] Both the forward and backward loads reduce its run length. Puzzlingly, the run length shows a dramatic asymmetry with respect to the direction of the load, with the run length under a medium forward load (e.g., with a magnitude of 2 pN–3 pN) being much smaller than that under the corresponding backward load.[21,22] Accordingly, the detachment rate also shows a dramatic asymmetry with respect to the loading direction.[21] While it is easy to explain the load-velocity relation, it is still difficult to understand how the detachment rate shows the dramatic asymmetry with respect to the loading direction.[9,21] The explanation of the origin of the dramatic asymmetry is critical to the molecular mechanism of the chemomechanical coupling of the kinesin motor.[9,21]

In addition, the experimental data from several research groups indicated that the detachment rate of the kinesin motor does not necessarily rise monotonically with the increase in the magnitude of the backward load.[15,21,32] The theoretical modeling also suggested that the detachment rate versus the magnitude of the backward load does not have the monotonic form.[9,33,34] On the contrary, according to Kramers theory, the detachment rate would increase exponentially with the increase in the magnitude of the load, as frequently assumed in the literature.[35–39] Determining the form of the detachment rate versus backward load is critically important to the theoretical or numerical studies of the cargo transport by the kinesin motors and in particular the transport by both the forward-moving kinesin and backward-moving dynein motors.[35–48]

To explain the dramatic asymmetry of the detachment rate of the kinesin motor with respect to the loading direction, two models have been proposed. One model was proposed by Xie,[49,50] which is called Model-I here, and the other one was proposed by Khataee and Howard,[51,52] which is called Model-II here. To verify which model is more reasonable, here we use the two models to study theoretically and numerically the dynamics of the kinesin motor versus the size of bead attached to the stalk for the case of the fixed trap in the optical trapping experiment and compare the theoretical/numerical results with the available experimental data.[30,31] In addition, to determine whether the detachment rate increases monotonically or not with the increase in the magnitude of the backward load, we also consider the model (called Model-III here), in which the detachment rate versus load has an exponential form, to study theoretically and numerically the

†Corresponding author. E-mail: pxie@iphy.ac.cn

© 2025 Chinese Physical Society and IOP Publishing Ltd. All rights, including for text and data mining, AI training, and similar technologies, are reserved.

dynamics of the motor versus bead size for the case of the fixed trap in the optical trapping experiment and compare the theoretical/numerical results with the available experimental data.[30,31]

2. Approximate theoretical analysis of maximal force and attachment duration

As done in the optical trapping experiment, we consider a large-sized bead attached to the motor stalk and a load, F_x, acts on the bead (Fig. 1). F_x is defined to be positive when it is in the backward direction. Due to the collision of the bead with MT in the assay, apart from the horizontal component (F_x) there also exists the vertical component (F_y) of the load, where the horizontal direction is parallel to the MT filament and the vertical direction is perpendicular to the MT filament. F_y can be written as

$$F_y = |F_x| \tan\Theta, \tag{1}$$

$$\Theta = \sin^{-1}\left[R_{\rm B}/(R_{\rm B}+l_{\rm S})\right], \tag{2}$$

where Θ is the angle of the stalk with respect to the MT filament, $R_{\rm B}$ is the bead radius and $l_{\rm S}$ is the stalk length. As done previously,[50–52] we take $l_{\rm S} = 35$ nm. The total magnitude of the load is

$$F = \left(F_x^2 + F_y^2\right)^{1/2}. \tag{3}$$

Note that here we only focus on the single motor attached to the bead. Under a backward load F_x, the bead is predominantly in the *xoy* plane. Although the fluctuation of the bead can cause it to deviate away from the *xoy* plane, resulting in the presence of the *z*-component (F_z) of the load, on average, F_z is approximately equal to zero and thus we do not consider F_z here.

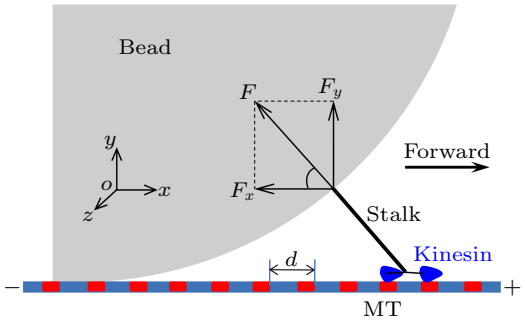


Fig. 1. Schematic diagram of a kinesin motor moving on an MT filament with a large-sized bead attached to the motor stalk and a backward load, F_x, on the bead.

In this section, we consider the case of the fixed trap in the optical trapping experiment, as done previously.[28] After the motor binds to the filament, the initial position of the motor is set as $x = 0$ and the motor is considered to be in the dwell period of the first mechanical step, when no load is present on the motor. Then, the motor steps forward processively. If during the *i*-th mechanical step the load on the motor is smaller than the stall force (*i* being an integer), the motor mainly steps forward and occasionally steps backward, where the stall force is defined as the load F_x under which the motor velocity becomes zero. Denoting by κ the trap stiffness, with κ having a very small value, during the *i*th mechanical step the load on the motor can be approximately written as $F_x(i) = \kappa(i-1)d$. Denoting by $v(i)$ the velocity under load $F_x(i) = \kappa(i-1)d$, the average dwell time of the *i*th mechanical step can be approximately computed with $d/v(i)$, where $d = 8$ nm is the step size equal to the repeat period of tubulin heterodimers on the MT filament. Notice that if during the *m*-th mechanical step $F_x(m) = \kappa(m-1)d$ becomes equal to the stall force (*m* being an integer, with $m > i$), $v(m) = 0$ and the dwell time of the *m*-th mechanical step is considered to be infinitely large if the motor is not detached.

Denote by $\varepsilon(i)$ the detachment rate of the motor during the *i*th mechanical step. Since during the *i*-th mechanical step the load on the motor is approximately $F_x(i) = \kappa(i-1)d$, $\varepsilon(i)$ is approximately equivalent to the detachment rate under load $F_x(i) = \kappa(i-1)d$. The detachment probability of the motor during the *i*-th mechanical step can then be approximately written as

$$P_i = \frac{\varepsilon(i)}{\varepsilon(i)+v(i)/d}. \tag{4}$$

The cumulative detachment probability of the motor after reaching the *n*-th mechanical step can be computed by $P_{\rm cum}^{(n)} = \sum_{i=1}^{n} P_i$ (*n* being an integer, with $n \le m$). With Eq. (4), $P_{\rm cum}^{(n)}$ can be rewritten as

$$P_{\rm cum}^{(n)} = \sum_{i=1}^{n} \frac{\varepsilon(i)}{\varepsilon(i)+v(i)/d}. \tag{5}$$

The average number of the mechanical steps, $n_{\rm max}$, that the motor can take before detachment can be obtained with cumulative detachment probability $P_{\rm cum}^{(n_{\rm max})} = 1$. The average maximal force that can be generated by the motor or the average force value at the termination of the force ramp, which is simply called maximal force, can be computed approximately by

$$F_{\rm max} = (n_{\rm max}-1)\,\kappa d. \tag{6}$$

The average attachment duration of the motor to MT, $t_{\rm dura}$, which is simply called attachment duration, can be approximately computed by

$$t_{\rm dura} = \sum_{i=1}^{n_{\rm max}} \tau(i), \tag{7}$$

where $\tau(i) = d/v(i)$ if $\varepsilon(i) < v(i)/d$ and $\tau(i) = 1/\varepsilon(i)$ if $\varepsilon(i) > v(i)/d$.

As it is seen from Eqs. (1)–(7), to compute $F_{\rm max}$ and $t_{\rm dura}$ it is required to know forms of the velocity v and detachment rate ε versus F_x. Different models would have different forms of v and ε versus F_x, which will be given in the following sections.

3. Dynamics of motor with Model-I

Model-I is described in detail in Sections S1, S2, and Fig. S1 in supporting information.[49,50] In Model I, a chemomechanical cycle of the motor can be divided into three periods during which the motor can detach with distinct rates. One is the weak MT-binding period (called period I), during which the motor is in one-head-bound (1HB) state, with one ADP-head binding to the local tubulin with a very weak affinity E_{w1}. Another one is also the weak MT-binding period (called period II), during which the motor is also in 1HB state, with one ADP-head binding to MT with a weak affinity E_{w2} ($\gg E_{w1}$). The third one is the strong MT-binding period (called strong period), during which the motor has at least one head binding strongly to MT with an affinity much larger than E_{w2}.

Based on the chemomechanical pathway (Fig. S1), the motor velocity at saturating ATP can be approximately written as[50]

$$v = [P_E k_T - (1-P_E) k_L] d, \tag{8}$$

$$k_T = \left(\frac{1}{k^{(+)}} + \frac{1}{k_{NL}}\right)^{-1} P_E + \left(\frac{1}{k_D} + \frac{1}{k^{(+)}} + \frac{1}{k_{NL}}\right)^{-1} (1-P_E), \tag{9}$$

$$k_L = \left(\frac{1}{k_D} + \frac{1}{k^{(-)}}\right)^{-1} P_E + k^{(-)} (1-P_E), \tag{10}$$

$$P_E = \frac{\exp\left(\frac{E_0 - F_x\delta}{k_B T}\right)}{\exp\left(\frac{E_0 - F_x\delta}{k_B T}\right) + 1}, \tag{11}$$

where k_T and k_L are ATPase rates of the trailing and leading heads, respectively, P_E is the probability of the trailing head taking a forward step after ATP transition to ADP in the head (see Fig. S1), $k^{(+)}$ and $k^{(-)}$ are rates of ATP transition to ADP in the head with its neck linker (NL) in the forward orientation and not in the forward orientation, respectively, k_D is the rate of ADP release from the MT-bound ADP-head, k_{NL} is the rate of the large conformational change of the ATP-head together with its NL docking and the reduction of its binding energy to the ADP-head in 1HB state, E_0 is the energy change associated with the large conformational change and NL docking of the ATP-head relative to the nucleotide-free head, δ is the distance parameter for the detached ADP-head to diffuse from the intermediate position in 1HB state to the nearest unoccupied tubulin, and $k_B T$ is the Boltzmann constant times the absolute temperature.

The expressions for the detachment rate are presented as follows. Under no or a backward load, the NL of the MT-bound ATP-head in 1HB state is not in the forward direction before NL docking, with the rate of ATP transition to ADP of the head given by

$$k = k^{(-)}, \quad \text{when} \quad F_x > 0. \tag{12}$$

Under a large forward load, the NL of the MT-bound head in 1HB state can be pulled in the loading orientation before NL docking, resulting in the NL severely clashing with a nucleotide-binding motif (a P-loop subdomain) in the nucleotide-free orientation to make the P-loop subdomain in the ATP-like orientation.[53] Thus, the rate of ATP transition to ADP of the MT-bound head becomes $k^{(+)}$. Therefore, under any forward load, the rate of ATP transition to ADP of the MT-bound head in 1HB state before NL docking can have following phenomenological form:[50]

$$k = k^{(-)} - \left(k^{(-)} - k^{(+)}\right)\left[1 - \exp\left(-\frac{|F_x|\,\delta_{NL}}{k_B T}\right)\right], \quad \text{when} \quad F_x < 0, \tag{13}$$

where δ_{NL} is the distance parameter for pulling NL of the MT-bound head in 1HB state in the loading direction before NL docking. Consequently, in an ATPase cycle, the occurrence probability of period I can be written as[50]

$$P_I = \frac{k}{k_{NL} + k}. \tag{14}$$

Since E_{w1} is very small, the detachment probability in period I is approximately $P_{dI} = 1$ under any load. In an ATPase cycle, the occurrence probability of period II can be written as[50]

$$P_{II} = P_E \frac{k^{(+)}}{k^{(+)} + k_D} + (1-P_E)\frac{k^{(-)}}{k^{(-)} + k_D}. \tag{15}$$

The detachment probability of the motor during period II is given by[50]

$$P_{dII} = \frac{k_{dII}}{k_{dII} + k_D}, \tag{16}$$

$$k_{dII} = \varepsilon_{w0} \exp\left(\frac{F\delta_w}{k_B T}\right), \tag{17}$$

where k_{dII} is the detachment rate in period II, ε_{w0} is the detachment rate under no load and δ_w is the distance parameter for the head to detach from MT by overcoming affinity E_{w2} in period II. Equation (17) is consistent with Kramers theory. For approximation, in the range of the load with the magnitude not very high ($|F_x| \leq 6$ pN), the detachment during the strong period can be neglected. Hence, the total detachment rate is given by[50]

$$\varepsilon = k_T P_I P_{dI} + (k_T + k_L) P_{II} P_{dII}. \tag{18}$$

Under the loads of very large magnitude ($|F_x| > 6$ pN), the detachment during the strong period should also be included. Since during the stepping cycle the motor is mainly in two-heads-bound state or strong period,[54] the total detachment rate under the loads of very large magnitude ($|F_x| > 6$ pN) can be approximately calculated by ε [Eq. (18)] plus $\varepsilon_s = \varepsilon_{s0} \exp[F\delta_s/(k_B T)]$, where ε_s is the detachment rate of the motor during the strong period, ε_{s0} is the unloaded detachment rate during the strong period, with $\varepsilon_{s0} \ll \varepsilon_{w0}$, and δ_s is the distance parameter for the motor to detach from MT during the

strong period. Note that ε_s increases exponentially with the increase of the load, according to Kramers theory.

As shown before,[50] using Eqs. (8)–(18) and taking parameter values listed in Table 1 under condition of Ref. [21] the theoretical results of the velocity, run length, detachment rate, and backward-stepping probability versus F_x in the range of $|F_x| \leq 6$ pN are in good agreement with the available experimental data for Drosophila kinesin.[21] The run length and detachment rate exhibit the dramatic asymmetry with respect to the loading direction. In the large range of $|F_x| > 6$ pN, with the total detachment rate being calculated by $\varepsilon + \varepsilon_s$ the theoretical results can also explain well the available experimental data for the load dependences of the velocity, run length, and detachment rate.[9,49]

Table 1. Parameter values for Drosophila kinesin used in Model-I. Values except for those with '*' are from Ref. [50]. Under condition of Refs. [30,31] for the fixed trap, parameter δ_{NL} is not required.

Parameter	Value under condition of Ref. [21]	Value under condition of Refs. [30,31]
$k^{(+)}$ (s^{-1})	101	101
$k^{(-)}$ (s^{-1})	3.6	3.6
k_D (s^{-1})	300	300
k_{NL} (s^{-1})	1500	1500
E_0 (k_BT)	3.6	3.6
δ (nm)	3.4	4.5*
ε_{w0} (s^{-1})	7	7
δ_w (nm)	1.1	2.2*
δ_{NL} (nm)	4	–

For the case of the fixed trap in the optical trapping experiment, since the maximal force is not very high ($F_x < 6$ pN), we can neglect the detachment during the strong period. Thus, we use forms of v and ε versus F_x given by Eqs. (8)–(18) to compute maximal force F_{max} and attachment duration t_{dura}, and compare the theoretical results with the experimental data of Pyrpassopoulos *et al.*[30,31] Similar to that used in the optical trapping experiment,[30,31] we take the trap stiffness $\kappa = 0.04$ pN/nm throughout. With the parameter values listed in Table 1 under condition of Ref. [21], the theoretical results of velocity versus F_x show that the stall force is about 8 pN (Fig. 2(a) for $\delta = 3.4$ nm). Since the parameter values listed in Table 1 were obtained by fitting Eqs. (8)–(11) to the experimental data of Andreasson *et al.*,[21] it is implied that under the experimental condition of Andreasson *et al.*[21] the stall force is about 8 pN. By comparisons, the experimental data of Pyrpassopoulos *et al.*[30,31] indicated that the stall force is about 6 pN. It is noted that by taking $\delta = 4.5$ nm (Table 1 under condition of Refs. [30,31]) and with all other parameters having the same values as listed in Table 1 under condition of Ref. [21], the stall force becomes about 6 pN (Fig. 2(a) for $\delta = 4.5$ nm). Thus, in order to compare the theoretical results with the experimental data of Pyrpassopoulos *et al.*,[30,31] we take $\delta = 4.5$ nm to compute F_{max} and t_{dura}. We take $k^{(+)}$, $k^{(-)}$, k_D, k_{NL}, E_0, and ε_{w0} having the same values as those listed in Table 1 under the condition of Ref. [21]. By adjusting only one parameter $\delta_w = 2.2$ nm (Table 1 under condition of Refs. [30,31]), using Eqs. (1)–(7) and with forms of v and ε versus F_x given by Eqs. (8)–(18), the theoretical results of both F_{max} and t_{dura} versus R_B are in agreement with the experimental data,[30,31] as shown in Figs. 2(b) and 2(c), where the data at $R_B = 0$ correspond to those measured using the three-beads assay. Moreover, we also show the corresponding numerical results of F_{max} and t_{dura} versus R_B in Figs. 2(b) and 2(c), which are obtained using the Monte–Carlo method (see Section S3 in supporting information), as used before.[38,55] It is seen that the numerical results are also consistent with the experimental data.

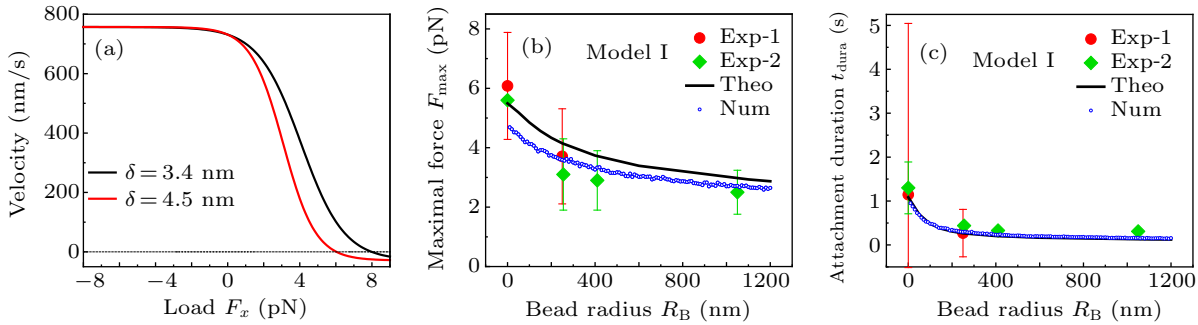


Fig. 2. Results with Model-I for the dynamics of kinesin motor. Lines are theoretical (Theo) results. Unfilled blue circles are numerical (Num) results. The experimental data in red dots (Exp-1) and green diamonds (Exp-2) are from Refs. [30,31], respectively, with $R_B = 0$ corresponding to the case of the three-beads assay. (a) Velocity versus load F_x. (b) Maximal force F_{max} versus bead radius R_B for the case of the fixed trap in the optical trapping experiment. (c) Attachment duration t_{dura} versus R_B for the case of the fixed trap in the optical trapping experiment.

In addition, from Eqs. (8)–(11) it is seen that the velocity v is independent of the vertical component F_y of the load. This is also consistent with the experimental data of Pyrpassopoulos *et al.*[30] showing that the average velocity values of about 300 nm/s for $R_B \geq 255$ nm and about 280 nm/s for $R_B = 0$ (corresponding to the case of the three-beads assay) are within 10% of each other under F_x below 3 pN. It is noted that these average velocity values are about 1.9-fold smaller than the average velocity value under F_x below 3 pN shown in Fig. 2(a) for $\delta = 4.5$ nm. To see how the variation of v affects F_{max} and t_{dura}, we reduce values of parameters $k^{(+)}$, $k^{(-)}$, k_D, and k_{NL} listed in Table 1 by 1.9-fold and with other values listed in Ta-

ble 1 under condition of Refs. [30,31] being unchanged. Note that reducing values of $k^{(+)}$, $k^{(-)}$, $k_{\rm D}$, and $k_{\rm NL}$ decreases only v but has no effect on the stall force (Fig. S2(a) in supporting information), as also noted from Eqs. (8)–(11). With these values the theoretical results of $F_{\rm max}$ and $t_{\rm dura}$ versus $R_{\rm B}$ are also in agreement with the experimental data of Pyrpassopoulos *et al.*,[30,31] as shown in Figs. S2(b) and S2(c) in supporting information.

Taken together, with Model-I the available experimental data on maximal force $F_{\rm max}$ and attachment duration $t_{\rm dura}$ versus bead radius for the case of the fixed trap in the optical trapping experiment are explained quantitatively. These support Model-I.

4. Dynamics of motor with Model-II

In Model-II, a stepping cycle of the motor is treated as consisting of three steps.[21,51] The expression for the load dependence of velocity is written as[21,51]

$$v=\frac{r_1^0 r_2^0 r_3^0 \exp\left[\dfrac{-F_x\sigma_1+(-F_x+F_{\rm i})\,\sigma_3}{k_{\rm B}T}\right]}{r_1^0 r_2^0 \exp\left(\dfrac{-F_x\sigma_1}{k_{\rm B}T}\right)+r_3^0 \exp\left[\dfrac{(-F_x+F_{\rm i})\,\sigma_3}{k_{\rm B}T}\right]\left[r_1^0 \exp\left(\dfrac{-F_x\sigma_1}{k_{\rm B}T}\right)+r_2^0\right]}d, \tag{19}$$

where $F_{\rm i}$ is the inter-head tension, r_1^0, r_2^0, and r_3^0 are rates of the three steps under no load, and σ_1, σ_2, and σ_3 are the corresponding distance parameters for the three rates. Note that $F_x>0$ when it is in the backward direction, as mentioned above. It should be mentioned that in Eq. (19) only the forward stepping is considered while the backward stepping is not included.

In Model-II, the motor detachment is assumed to consist of two kinetic steps. In other words, the detachment passes through three states: strong MT-binding state $\xrightarrow{k_1}$ weak MT-binding state $\xrightarrow{k_2}$ detached state.[51,52] Thus, the detachment rate is written as

$$\varepsilon=\frac{k_1k_2}{k_1+k_2}. \tag{20}$$

Additionally, it is assumed that the vertical component F_y of the load increases the detachment rate and the forward horizontal component F_x (<0) also increases the detachment rate, which is consistent with Kramers theory, whereas the backward horizontal component F_x (>0) decreases the detachment rate, which is contrary to Kramers theory. However, the assumption of the backward horizontal force decreasing the detachment rate is puzzling, the origin of which is still needed to investigate if it is correct. According to the assumption, the load dependences of k_1 and k_2 are written as[51,52]

$$k_1=k_1^0\exp\left(\frac{-F_x\delta_{x1}+F_y\delta_{y1}}{k_{\rm B}T}\right), \tag{21}$$

$$k_2=k_2^0\exp\left(\frac{-F_x\delta_{x2}+F_y\delta_{y2}}{k_{\rm B}T}\right), \tag{22}$$

where k_1^0 and k_2^0 are rates of k_1 and k_2 under no load, respectively, δ_{x1} and δ_{y1} are distance parameters for rate k_1 in the horizontal and vertical directions, respectively, and δ_{x2} and δ_{y2} are distance parameters for rate k_2 in the horizontal and vertical directions, respectively.

As shown before,[51] by fitting Eqs. (19)–(22) to the experimental data on the velocity and detachment rate versus F_x for Drosophila kinesin measured by Andreasson *et al.* using $R_{\rm B}=220$ nm,[21] the obtained parameter values are listed in Table 2. The theoretical results show that the detachment rate exhibits the dramatic asymmetry with respect to the loading direction. The asymmetry arises solely from the assumption that the horizontal component F_x of the forward load increases whereas that of the backward load decreases the detachment rate ε, because the vertical component F_y of the forward load and that of the backward load have the same effect on ε. However, the theoretical results show that the detachment rate has a slip-bonding or exponential form under both forward and backward loads, which is inconsistent with the available experimental evidence of the slip-catch-slip-bonding form for the detachment versus backward load.[15,21,32]

Here, we use forms of v and ε versus F_x given by Eqs. (19)–(22) to compute maximal force $F_{\rm max}$ and attachment duration $t_{\rm dura}$ for the case of the fixed trap in the optical trapping experiment and compare the theoretical results with the experimental data of Pyrpassopoulos *et al.*[30,31] With the parameter values listed in Table 2, using Eqs. (1)–(7) the theoretical results of $F_{\rm max}$ and $t_{\rm dura}$ versus bead radius $R_{\rm B}$ are shown in Figs. 3(a) and 3(b). Moreover, we also show the corresponding numerical results of $F_{\rm max}$ and $t_{\rm dura}$ versus $R_{\rm B}$ in Figs. 3(a) and 3(b), which are obtained using the Monte–Carlo method described in Section S3. It is seen that both $F_{\rm max}$ and $t_{\rm dura}$ increase significantly with the decrease of $R_{\rm B}$. At small $R_{\rm B}$, $F_{\rm max}$ and $t_{\rm dura}$ are much larger than the experimental data. For example, at $R_{\rm B}=0$, the theoretical/numerical value of $F_{\rm max}$ is more than 2-fold larger than the experimental value and the theoretical/numerical value of $t_{\rm dura}$ is more than 10^4-fold larger than the experimental value. This is understandable easily, because in Model-II it is assumed that at $R_{\rm B}=0$, implying $F_y=0$, the detachment rate decreases exponentially with the increase of F_x when F_x is large, as noted from Eqs. (20)–(22) and parameter values listed in Table 2.

Table 2. Parameter values for Drosophila kinesin used in Model-II. Values are from Refs. [21,51,52].

Parameter	$F_{\rm i}$ (pN)	r_1^0 (s^{-1})	r_2^0 (s^{-1})	r_3^0 (s^{-1})	σ_1 (nm)	σ_2 (nm)	σ_3 (nm)	k_1^0 (s^{-1})	k_2^0 (s^{-1})	δ_{x1} (nm)	δ_{y1} (nm)	δ_{x2} (nm)	δ_{y2} (nm)
Values	26	4900	95	260	4.6	0	0.35	0.91	7.62	2.9	2.25	0	0.18

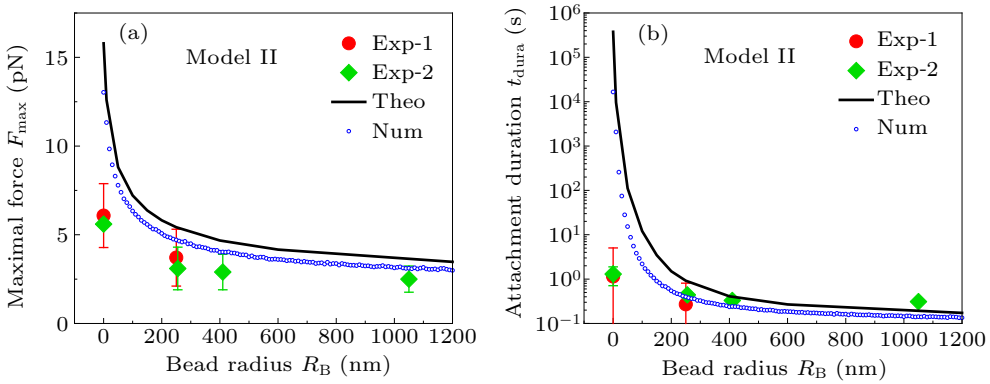


Fig. 3. Results with Model-II for maximal force $F_{\rm max}$ and attachment duration $t_{\rm dura}$ versus bead radius $R_{\rm B}$ for the case of the fixed trap in the optical trapping experiment. Lines are theoretical results. Unfilled blue circles are numerical results. The experimental data in red dots (Exp-1) and green diamonds (Exp-2) are from Refs. [30,31], respectively, with $R_{\rm B}=0$ corresponding to the case of the three-beads assay. (a) $F_{\rm max}$ versus $R_{\rm B}$, (b) $t_{\rm dura}$ versus $R_{\rm B}$.

Taken together, with Model-II the theoretical/numerical results on maximal force $F_{\rm max}$ and attachment duration $t_{\rm dura}$ versus bead radius $R_{\rm B}$ for the case of the fixed trap in the optical trapping experiment deviate significantly away from the experimental data. These argue against Model-II.

5. Dynamics of motor with Model-III

In Model-III, it is assumed that the detachment rate versus backward load has the slip-bonding form. According to Kramers theory, the detachment rate versus the total magnitude of the load has the exponential form

$$\varepsilon = \varepsilon_0 \exp\left(\frac{F\delta_0}{k_{\rm B}T}\right), \tag{23}$$

where ε_0 is the detachment rate under no load, δ_0 is the distance parameter and F as a function of F_x has the form described by Eqs. (1)–(3).

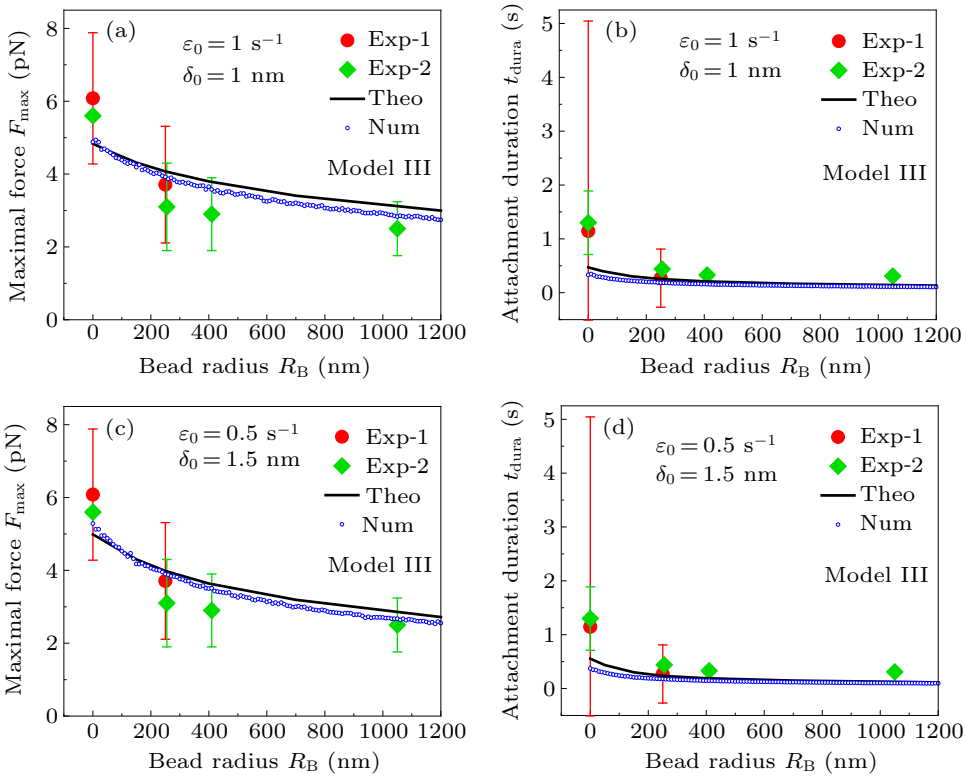


Fig. 4. Results with Model-III for maximal force $F_{\rm max}$ and attachment duration $t_{\rm dura}$ versus bead radius $R_{\rm B}$ for the case of the fixed trap in the optical trapping experiment. Lines are theoretical results. Unfilled blue circles are numerical results. The experimental data in red dots (Exp-1) and green diamonds (Exp-2) are from Refs. [30,31], respectively, with $R_{\rm B}=0$ corresponding to the case of the three-beads assay. (a)–(b) $F_{\rm max}$ and $t_{\rm dura}$ versus $R_{\rm B}$ for $\varepsilon_0=1$ s^{-1} and $\delta_0=1$ nm; (c)–(d) $F_{\rm max}$ and $t_{\rm dura}$ versus $R_{\rm B}$ for $\varepsilon_0=0.5$ s^{-1} and $\delta_0=1.5$ nm.

We use the form of ε versus F_x given by Eqs. (1)–(3) and (23) and still use the form of v versus F_x given by Eqs. (8)–(11) to compute maximal force $F_{\max}$ and attachment duration $t_{\rm dura}$ for the case of the fixed trap in the optical trapping experiment and compare the theoretical results with the experimental data of Pyrpassopoulos *et al.*[30,31] As done in Fig. 2(a), we use values of parameters $k^{(+)}$, $k^{(-)}$, $k_{\rm D}$, $k_{\rm NL}$, E_0, and δ listed in Table 1 under condition of Refs. [30,31] to determine the form of v versus F_x. As the available experimental data showed that the detachment rate under no load, ε_0, is about 0.8 $\rm s^{-1}$,[21] we take two values of ε_0, namely $\varepsilon_0 = 1$ $\rm s^{-1}$ and $\varepsilon_0 = 0.5$ $\rm s^{-1}$, to make the computation. We adjust parameter δ_0 to make the theoretical results be best fit to the experimental data. Using Eqs. (1)–(7) the theoretical results of $F_{\max}$ and $t_{\rm dura}$ versus $R_{\rm B}$ with $\delta_0 = 1$ nm are shown in Figs. 4(a) and 4(b) and with $\delta_0 = 0.5$ nm are shown in Figs. 4(c) and 4(d). Moreover, we also show the corresponding numerical results of $F_{\max}$ and $t_{\rm dura}$ versus $R_{\rm B}$ in Fig. 4, which are obtained using the Monte–Carlo method described in Section S3 of supporting information.

By comparing Fig. 2 with Fig. 4 it is seen that the theoretical/numerical results with Model-I show better agreement with the experimental data than with Model-III. Concretely, the theoretical/numerical results of $t_{\rm dura}$ versus $R_{\rm B}$ with Model-III (Figs. 4(c) and 4(d)) show that as $R_{\rm B}$ decreases from 250 nm to 0, $t_{\rm dura}$ has only a small increase, whereas the experimental data showed that as $R_{\rm B}$ decreases from 250 nm to 0, $t_{\rm dura}$ increases largely. By contrast, both the theoretical/numerical results with Model-I and the experimental results of $t_{\rm dura}$ versus $R_{\rm B}$ (Fig. 2(c)) show that as $R_{\rm B}$ decreases from 250 nm to 0, $t_{\rm dura}$ increases largely, and as $R_{\rm B}$ increases from 250 nm to 1050 nm, $t_{\rm dura}$ decreases slightly. This thus indicates that Model-I is more applicable to describing the dependence of the detachment rate upon load than Model-III. In other words, it is more probable that the detachment rate of the kinesin motor versus backward load has a non-slip-bonding rather than the simple exponential (or slip-bonding) form.

6. Conclusion

Using Model-I, Model-II, and Model-III, we studied theoretically and numerically the maximal force $F_{\max}$ and attachment duration $t_{\rm dura}$ of the kinesin motor versus bead radius $R_{\rm B}$ for the case of the fixed trap in the optical trapping experiment. We compared the theoretical/numerical results with the available experimental data. It is shown that the theoretical/numerical results obtained using Model-I agree well with the experimental data, whereas those using Model-II deviate significantly away from the experimental data. The significant deviation of the theoretical/numerical results obtained using Model-II from the experimental data is due to the assumption that the detachment rate decreases exponentially with the increase in the horizontal component F_x of the backward load.[51,52] When the bead radius $R_{\rm B}$ is small only the horizontal component F_x is predominant. Thus, as $R_{\rm B}$ decreases, the detachment rate decreases largely, giving the significant increase of both the attachment duration $t_{\rm dura}$ and maximal force $F_{\max}$ compared to the experimental data. By contrast, in Model I the detachment rate increases but does not increase monotonously with the increase of F_x,[49,50] giving the theoretical/numerical results of $t_{\rm dura}$ and $F_{\max}$ versus $R_{\rm B}$ consistent with the experimental data. This indicates that Model-I is applicable whereas Model-II is not applicable to the description of the load dependence of the detachment rate. Using Model-I the theoretical/numerical results are in better agreement with the experimental data than using Model-III. This is because in Model-III the detachment rate is simply assumed to increase exponentially or monotonously with the increase of the load whereas in Model-I the detachment rate does not increase monotonously with the increase of the load. This indicates that the detachment rate versus backward load exhibits most probably a non-slip-bonding rather than an exponential form.

Acknowledgement

Project supported by Youth Project of Science and Technology Research Program of Chongqing Education Commission of China (Grant No. KJQN202404522).

References

[1] Vale R D, Reese T S and Sheetz M P 1985 *Cell* **42** 39
[2] Kozielski F, Sack S, Marx A, *et al.* 1997 *Cell* **91** 985
[3] Howard J 2001 *Mechanics of Motor Proteins and the Cytoskeleton* (Sunderland, MA, USA: Sinauer Associates)
[4] Vale R D 2003 *Cell* **112** 467
[5] Lawrence C J, Dawe R K, Christie K R, *et al.* 2004 *J. Cell Boil.* **167** 19
[6] Miki H, Okada Y and Hirokawa N 2005 *Trends Cell Biol.* **15** 467
[7] Hirokawa N, Noda Y, Tanaka Y, *et al.* 2009 *Nat. Rev. Mol. Cell Bio.* **10** 682
[8] Vale R D and Milligan R A 2000 *Science* **288** 88
[9] Xie P 2021 *Commun. Theor. Phys.* **73** 057601
[10] Wang J G, Shi X X, Liu Y R, *et al.* 2022 *Chin. Phys. B* **31** 058702
[11] Geng Y Z, Lu L A, Jia N, *et al.* 2023 *Chin. Phys. B* **32** 108701
[12] Liu Y and Zhang Z 2024 *Chin. Phys. B* **33** 028708
[13] Svoboda K, Schmidt C F, Schnapp B J, *et al.* 1993 *Nature* **365** 721
[14] Schnitzer M J and Block S M 1997 *Nature* **388** 386
[15] Coppin C M, Pierce D W Hsu L, *et al.* 1997 *Proc. Natl. Acad. Sci. USA* **94** 8539
[16] Kojima H, Muto E, Higuchi H, *el al.* 1997 *Biophys. J.* **73** 2012
[17] Visscher K, Schnitzer M J and Block S M 1999 *Nature* **400** 184
[18] Nishiyama M, Higuchi H and Yanagida T 2002 *Nat. Cell Biol.* **4** 790
[19] Khalil A S, Appleyard D C, Labno A K, *et al.* 2008 *Proc. Natl. Acad. Sci. USA* **105** 19247
[20] Carter N J and Cross R A 2005 *Nature* **435** 308
[21] Andreasson J O L, Milic B, Chen G Y, *et al.* 2015 *eLife* **4** e07403
[22] Milic B, Andreasson J O L, Hancock W O, *et al.* 2014 *Proc. Natl. Acad. Sci. USA* **111** 14136
[23] Xie P 2022 *Eur. Phys. J. E* **45** 28

[24] Mehta A D, Rock R S, Rief M, *et al*. 1999 *Nature* **400** 590
[25] Uemura S, Higuchi H, Olivares A O, *et al*. 2004 *Nat. Struct. Mol. Biol.* **11** 877
[26] Rief M, Rock R. S., Mehta A D, *et al*. 2000 *Proc. Natl. Acad. Sci. USA* **97** 9482
[27] Clemen A E M, Vilfan M, Jaud J, *et al*. 2005 *Biophys. J.* **88** 4402
[28] Xie P 2024 *Cell. Mol. Bioeng.* **17** 137
[29] Budaitis B G, Jariwala S, Rao L, *et al*. 2021 *J. Cell Biol.* **220** e202004227
[30] Pyrpassopoulos S, Shuman H and Ostap E M 2020 *Biophys. J.* **118** 243
[31] Pyrpassopoulos S, Gicking A M, Zaniewski T M, *et al.* 2023 *Proc. Natl. Acad. Sci. USA* **120** e2216903120
[32] Kunwar A, Tripathy S K, Xu J, *et al*. 2011 *Proc. Natl. Acad. Sci. USA* **108** 18960
[33] Bouzat S and Falo F 2010 *Phys. Biol.* **7** 046009
[34] Guo S K, Shi X X, Wang P Y, *et al.* 2019 *Biophys. Chem.* **253** 106216
[35] Vu H T, Chakrabarti S, Hinczewski M, *et al*. 2016 *Phys. Rev. Lett.* **117** 078101
[36] Berger F, Keller C, Klumpp S, *et al*. 2012 *Phys. Rev. Lett.* **108** 208101
[37] Berger F, Keller C, Lipowsky R, *et al*. 2013 *Cell. Mol. Bioeng.* **6** 48
[38] Wang Y, Liu Y Y, Liang J, *et al*. 2021 *Commun. Theor. Phys.* **73** 15603
[39] Bameta T, Das D, Das D, *et al*. 2017 *Phys. Rev. E* **95** 22406
[40] Fernández Casafuz A B, De Rossi M C and Bruno L 2020 *Phys. Rev. E* **101** 62416
[41] Kunwar A, Vershinin M, Xu J, *et al*. 2008 *Curr. Biol.* **18** 1173
[42] Arpağ G, Shastry S, Hancock W O, *et al*. 2014 *Biophys. J.* **107** 1896
[43] Uçar M C and Lipowsky R 2020 *Nano Lett.* **20** 669
[44] Muller M J, Klumpp S and Lipowsky R 2008 *Proc. Natl Acad. Sci. USA* **105** 4609
[45] Fu Y B, Guo S K, Wang P Y, *et al*. 2019 *Eur. Phys. J. E* **42** 41
[46] Dallon J C, Leduc C, Etienne-Manneville S, *et al*. 2019 *J. Theor. Biol.* **464** 132
[47] Portet S, Etienne-Manneville S, Leduc C, *et al*. 2022 *J. Theor. Biol.* **547** 111183
[48] Wang Y, Liu Y, Wang P, *et al*. 2022 *Commun. Theor. Phys.* **74** 105601
[49] Xie P 2020 *ACS Omega* **5** 5721
[50] Xie P 2021 *J. Theor. Biol.* **530** 110879
[51] Khataee H and Howard J 2019 *Phys. Rev. Lett.* **122** 188101
[52] Khataee H, Mahamdeh M and Neufeld Z 2020 *Phys. Rev. E* **102** 022406
[53] Cao L, Wang W, Jiang Q, *et al*. 2014 *Nat. Comm.* **5** 5364
[54] Xie P 2024 *J. Phys. Chem. Lett.* **15** 3893
[55] Wang Y, Liu Y R, Wang P Y, *et al*. 2024 *J. Phys. Chem. B* **128** 1194